Chemical Science

ROYAL SOCIETY OF CHEMISTRY

PERSPECTIVE

View Article Online
View Journal | View Issue

Cite this: *Chem. Sci.*, 2021, **12**, 10410

All publication charges for this article have been paid for by the Royal Society of Chemistry

Received 21st April 2021
Accepted 5th July 2021

DOI: 10.1039/d1sc02236a

rsc.li/chemical-science

Azanone (HNO): generation, stabilization and detection

Cecilia Mariel Gallego,† Agostina Mazzeo,† Paola Vargas,† Sebastián Suárez, Juan Pellegrino and Fabio Doctorovich *

HNO (nitroxyl, azanone), joined the 'biologically relevant reactive nitrogen species' family in the 2000s. Azanone is impossible to store due to its high reactivity and inherent low stability. Consequently, its chemistry and effects are studied using donor compounds, which release this molecule in solution and in the gas phase upon stimulation. Researchers have also tried to stabilize this elusive species and its conjugate base by coordination to metal centers using several ligands, like metalloporphyrins and pincer ligands. Given HNO's high reactivity and short lifetime, several different strategies have been proposed for its detection in chemical and biological systems, such as colorimetric methods, EPR, HPLC, mass spectrometry, fluorescent probes, and electrochemical analysis. These approaches are described and critically compared. Finally, in the last ten years, several advances regarding the possibility of endogenous HNO generation were made; some of them are also revised in the present work.

1. Introduction

Nitric oxide, NO˙, was initially known for being one of the environmentally polluting gasses. Since its identification as an endogenous molecule in humans as the endothelium derived relaxing factor (EDRF),[1] countless studies followed to shed light on its important role in biological systems. Nowadays, it is well known, for example, that NO˙ is capable of selectively activating enzymes such as soluble guanylate cyclase (sGC), generating an increase in cyclic guanosine monophosphate (cGMP) levels, leading to cGMP-dependent signalling pathways.[2] Azanone (HNO, nitroxyl), the one electron reduced and protonated congener of nitric oxide, also reacts with O_2, thiols, hemoproteins, and transition metals. However, their overall chemical reactivity is different. For example, in aqueous solution, HNO dimerizes with a second-order rate constant of approximately 8×10^6 M^{-1} s^{-1} to produce hyponitrous acid, which eventually decomposes to produce nitrous oxide and water,[3] making HNO detection difficult. There is evidence for very little NO dimerization in the gas state. However, in solution, or inside solid materials, the story might be different. For example, when confined within nanoporous carbon, nitric oxide is found to react completely to form the dimer, $(NO)_2$, even though almost no dimers are present in the bulk gas phase in equilibrium with the pore phase.[4] Houk *et al.* presented theoretical evidence for the role of the NO dimer in reactions of NO with nucleophiles, showing that the concentration of $(NO)_2$ increases in aromatic environments.[5] Also, properties predicted by theoretical studies were in excellent agreement with experimental studies based on Infrared and Raman spectroscopy in the gas phase.[6]

HNO and NO˙ also react with each other, with a second-order rate constant of 6×10^6 M^{-1} s^{-1}.[7] Besides, HNO can be converted to NO˙ by relatively mild hydrogen atom abstractors, since the H–NO bond strength is only ~50 kcal mol^{-1},[8] making it a better hydrogen atom donor than many other biological antioxidants. Indeed, HNO is a potent antioxidant due to its ability to react with oxidizing radicals and generating NO˙,[9] which can also react with and quench reactive radical species. Moreover, it has been established that HNO is capable of rapidly reducing a variety of biological oxidants including hemoproteins,[10] metalloenzymes (such as superoxide dismutase),[11] and flavins[12] to give NO˙. In the last ten years, the reactions between HNO and several physiological species were studied.[13,14] In all cases, the second-order rate constants were obtained with values ranging between 10^3 and 10^5 M^{-1} s^{-1}.

Historically, direct HNO formation from the chemical reduction of NO˙ seemed unlikely to occur due to the rather negative reduction potential; however, this value is currently under review. Rocha *et al.* computed $E^{\circ\prime}$ (NO˙, H^+/HNO) = −0.161 V *versus* NHE at pH = 7,[15] so, in this context, NO˙ could be reduced by biologically compatible species with reduction potentials between −0.3 and −0.5 V. The more negative redox potential of −0.55 V at pH 7 was derived in 2002 by Shafirovich and Lymar,[3] by using $\Delta_f G^\circ(NO_{aq})$, the gas phase enthalpy of formation for ^{1}HNO, the tabulated entropy $S^\circ(HNO_{gas})$ and approximations for free energy of formation of HNO in aqueous solution, $\Delta_f G^\circ(^1HNO_{aq})$. In 2017 an efficient protocol was

Departamento de Química Inorgánica, Analítica, y Química Física, Facultad de Ciencias Exactas y Naturales, Universidad de Buenos Aires, INQUIMAE-CONICET, Ciudad Universitaria, Pab. 2, C1428EHA, Buenos Aires, Argentina. E-mail: doctorovich@qi.fcen.uba.ar

† These authors contributed equally.

Table 1 Comparative summary of the relevant chemistry of HNO *vs.* NO$^{\bullet}$

	HNO	NO$^{\bullet}$
Production	NOS byproduct RSNO decomposition NH_2OH oxidation NO reduction	NOS
Direct effect – molecular targets	Thiols Metal complexes (specially Fe^{3+})	Free radicals Metal complexes (specially Fe^{2+})
Indirect effects	Formation of oxidative species from reaction with O_2	RNOS formation: NO_2, N_2O_3 and $ONOO^-$
Physiological activity	Vasodilation Neuromodulation and neurotoxic in CNS Favours myocardial contraction Protection against ischemia/reperfusion injuries	Macrophage and immune response activation Mitochondrial hemeprotein regulation

derived to obtain the solvation free energy of HNO using three different computational approaches.[17] Therefore −0.161 V is probably a more exact value for $E^{\circ\prime}$ (NO$^{\bullet}$, H^+/HNO).

Both HNO and NO$^{\bullet}$ share many pharmacological effects related to the cardiovascular system,[16] and respiratory diseases[17] among others. However, the biochemical pathways through which they act are quite different. A comparative summary of their biologically relevant chemisry is shown in Table 1. It is well established that NO$^{\bullet}$ maintains normal cardiovascular functions *via* the activation of the sGC enzyme. In the case of HNO, it emerged as a possible biologically active compound in the mid-1980s due to studies related to cyanamide (H_2NCN), a drug used to treat alcoholism.[18] In a series of studies, cyanamide was shown to be oxidatively bioactivated (for example, by catalase/H_2O_2) to generate HNO that, in turn, was responsible for the inhibition of aldehyde dehydrogenase *via* modification of the cysteine thiolate active site. Further work showed that HNO released *via* cyanamide also resulted in vasorelaxation in rabbit thoracic aorta.[19] Although it is debatable whether HNO is also an endogenously generated EDRF, it has also been proposed that HNO could be an endothelium-derived hyperpolarizing factor (EDHF).[20]

More recently, HNO has been shown to irreversibly hinder the activity of the enzyme glyceraldehyde 3-phosphate dehydrogenase (GAPDH). This makes HNO a possible anticancer agent, since most solid tumours use glycolysis as their main source of energy. Furthermore, recent studies show that breast cancer cells are affected by the presence of azanone through their interaction with the poly(ADPRibose) polymerase inhibitor (PARP).[21] In addition to these biological effects, HNO has also been shown to affect mycobacterium tuberculosis growth by interfering with its general physiological state.[22]

Another therapeutic application for HNO in the cardiovascular system is its use as a powerful preconditioning agent, which helps to alleviate the negative consequences of an ischemic event and the consequent reperfusion injury. This injury is characterized by blood flow deprivation followed by necrosis and possible heart tissue hypoxia. Animal studies show that a dramatic decrease in infarct size was achieved by pre-treating heart tissue with Angeli's salt (an HNO donor); however, HNO has also been shown to increase infarct size if administered during an ischemic event.[23]

Information on HNO donors that are in clinical trials for heart failure treatments is currently publicly available (Scheme 1).[24] Cimlanod (BMS-986231, CXL-1427) represents a second generation donor that delivers HNO through a pH-dependent chemical breakdown when exposed to the neutral pH environment of the bloodstream, and as a consequence, generates positive lusitropic and inotropic effects, as well as vasodilator effects.[25] CXL-1020 is a first-generation HNO donor that generates an inactive organic by-product, CXL-105. It was shown to produce beneficial vasodilatory, inotropic, and lusitropic effects in normal and heart failure animal models; however, due to injection-site toxicity, its development was halted.[26]

Finally, a recent discovery on the pharmacological effects of HNO focusing on diabetes-related complications of the cardiovascular system was published.[27] Oxidative stress induced by hyperglycemia impairs both endogenous NO$^{\bullet}$ generation and its response capacity within the myocardium, which leads to complications for traditional NO$^{\bullet}$ therapies. However, the inotropic and lusotropic responses to HNO are enhanced, demonstrating the potential role for therapeutic HNO administration in acute treatment of ischemia and/or heart failure in diabetics.

In this account, the latest achievements on HNO generation, coordination chemistry and detection will be reviewed, with special focus on contributions made by our group.

2. HNO generation

2.1 Solution

Until 2015, although HNO formation from the reaction of NO$^{\bullet}$ with alcohols had been considered, for example, using oxidized polyolefins,[28] ubiquinol[29] and 3,4-dihydroxyphenylacetic acid

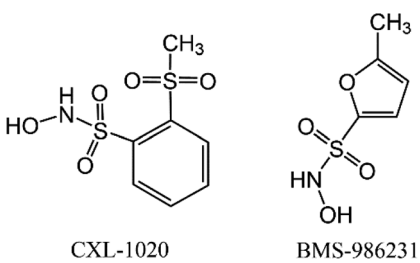

Scheme 1 Structures of HNO-donors currently in medical trials.

Table 2 k_{eff} and N_2O : nitrite ratio obtained for the reactions of NO with reducing agents

Compound	Functional group	k_{eff}[a] (M^{-1} s^{-1})	NO_2^-: N_2O[b]	Ref.
Benzenethiol	–SH	110 ± 8	1.0	40
Cysteine		25 ± 6	1.2	40
BSA[c]		0.6	—	42
H_2S		6300 ± 300	1.0	39
Ascorbic acid	–OH	8.1 ± 0.4	1.2	31
Hydroquinone		6.0 ± 0.4	1.2	31
α-Tocopherol		3.3 ± 0.4	—	32
Acetaminophen		1.4 ± 0.6	—	32
Piroxicam		0.26 ± 0.04	—	32
Isopropylamine	$–NH_2$	0.070 ± 0.007	1.0	41
Diethylamine	–NH	0.030 ± 0.005	1.2	41

[a] pH = 7.4, RT, anaerobic, in the presence of DPTA (diethylenetriaminepentaacetic acid). [b] Estimated error is (±0.1). [c] Bovine serum albumin (BSA) is a high molecular weight protein ($M_r \approx 7 \times 10^4$) that has only one free thiol group.

(DOPAC);[30] none of these studies provided its direct, unequivocal detection. Recently, we studied the reaction of NO• with aromatic and pseudoaromatic alcohols, the ascorbate anion ($AscH^-$), phenol (PhOH), hydroquinone (HQ), and tyrosine (Y) through several approaches.[31] The reaction occurred after mixing NO• with ascorbate and aromatic alcohols, but not with aliphatic ones like methanol, D-mannitol, or malic acid. HNO concentration was linearly dependent on both ROH and NO concentrations; the resulting bimolecular constants (k_{eff}) are reported in Table 2. Data shows that the diols (hydroquinone and ascorbate) react approximately five-ten times faster than phenols, with ascorbate being the fastest. Alcohol-derived radicals were detected as reaction intermediates by EPR spectroscopy. Additionally, we decided to inspect whether other vitamins bearing phenolic groups, such as α-tocopherol (vitamin E, absorbed and accumulated in humans), or over-the-counter medications, such as acetylsalicylic acid (aspirin) or acetaminophen (paracetamol), can undergo the reaction.[32] We found that all three species are capable of producing HNO from NO•. Aspirin, an aromatic acetyl ester, although initially incapable of reacting with NO• due to its protected –OH group, is transformed in the stomach into salicylic acid, whose reactivity towards NO• could be demonstrated. Piroxicam also produced HNO after reacting with NO•.

From these results, we proposed that these reactions occur *via* a proton-coupled nucleophilic attack (PCNA) by the alcohol on NO•, producing an intermediate RO–N(H)O• species, which further decomposes to release HNO (Scheme 2).

HNO, in turn, reacts with NO• to give nitrite, and with itself to give N_2O.[33] (eqn (1))

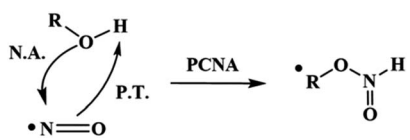

Scheme 2 PCNA mechanism. PCNA: proton-coupled nucleophilic attack, P.T.: proton transfer, N.A.: nucleophilic attack.

$$2HNO(g) \rightarrow N_2O(g) + H_2O(l) \quad (1)$$

The alkoxyl radicals, on the other hand, may react with another equivalent radical, such as tyrosine, which produces dityrosine, or with a second NO• molecule to produce an *O*-nitroso compound, as is the case for diols like ascorbate or hydroquinone.

Another question that arises regarding HNO generation is whether its production from the reaction of NO• with dihydrogen sulfide (H_2S) and thiols is possible. H_2S is a small gasotransmitter molecule, which has been shown to have cardioprotective effects on its own.[34,35]

We observed that HNO formation is first order in both reactants, H_2S and NO. The reaction between these compounds could proceed *via* a direct one-electron transfer, promoting the reduction of NO• to HNO or, alternatively, HS^- could attack NO in a proton-coupled nucleophilic attack to form $HSNO^{\bullet-}$, as reported for the reaction of NO with alcohols.[36] This contrasts with the studies performed by Cortese–Krott, who proposed that the main product of the direct reaction was $SSNO^-$, evidenced by an absorption maximum at 412 nm.[37] Recently, however, *via* the transnitrosation reaction (RSNO + R′SH ⇄ R′SNO + RSH), Marcolongo *et al.* observed that an absorption band at 412 nm reaches its full development one minute after mixing the RSNO/HS^- reagents. Simultaneously, the appearance of NO• is observed after the initial RSNO reagent has already disappeared. From these data and the evidence that {(H)SNO} has a half-life of six seconds, they concluded that {(H)SNO} is the first intermediate in the transnitrosation reaction, and a precursor for $SSNO^-$.[38] Both the development of the absorption band at 412 nm following the reaction between H_2S and NO•, which depends on HS^- concentration, and the delayed release of NO• are consistent with $SSNO^-$ formation. For more detail and discussion on the reactivity and interconversion of these nitrogen and sulfur species, the reader is referred to more specific works.[38,39]

On the other hand, previous studies showed that NO• can also react with thiols, leading to the formation of disulfides, N_2O, and, finally, N_2.[30] In this context, we approached the reaction of NO• with thiols the same way as we did for alcohols.[40] For this analysis, the reactions of NO• with 1-hexanethiol (R_6-SH), cysteine (Cys), benzenethiol (Ph-SH), and benzeneselenol (Ph-SeH), were evaluated. The results revealed that HNO production rate varies in the following order: Ph-SeH > Ph-SH ≫ R_6-SH > Cys. We also confirmed that the reaction is first order in both reagents. Cys and R_6-SH, both aliphatic thiols, display similar reactivity, with effective rate constants approximately four times smaller than those observed for Ph-SH and Ph-SeH. This is because aromatics allow better stabilization of the unpaired spin.

Finally, in a similar way, we studied the reaction between alkylamines and NO•.[41] However, the obtained k_{eff} values for HNO production were between twenty and two hundred fifty times smaller than those obtained for other moderate NO• reducing agents (at pH 7.4). In all cases, the results presented in Table 2 show that N_2O and NO_2^- are produced in approximately a 1 : 1 ratio, as expected considering the reaction between HNO and NO• (2):

$$2NO^{\bullet} + HNO \rightarrow N_2O \text{ and } NO_2^- + N_2O + H^+ \quad (2)$$

2.2 HNO donors

Azanone is impossible to store due to its high reactivity and inherent low stability. In consequence, its chemistry and effects are studied using HNO donor compounds, which release this molecule upon certain stimulation (chemical, photochemical, or thermal). For example, Angeli's Salt ($Na_2N_2O_3$) releases HNO (and nitrite) at acidic pH (Scheme 3a), while there are many base-catalyzed donors, like Piloty's acid derivatives and pyrazolone-based compounds such as HAPY-1 (4-(*N*-hydroxylamino)-4-(acetyl-*O*-methyoxyoxime)-*N*-phenyl-3-methylpyrazolone) (Scheme 3b and c respectively).

In 2017, we showed that HNO release can be photochemically induced by irradiating Piloty's acid solutions with visible light in the presence of a Ru-bpy complex as an actuator.[43] When the Ru complex is irradiated with visible light, amine ligands are released, increasing the pH of the solution. This, in turn, activates HNO release from Piloty's acid derivatives as discussed above. Light-driven azanone release had been previously reported using *N*-alkoxysulfonamide donors and Xe light irradiation.[44] In this case, HNO was released due to an uncaging mechanism and not because of a pH shift. Other examples for photochemical HNO release have also been reported based on the same family of donors,[45,46] caged Piloty's acid,[47] and even $\{FeNO\}^6$ complexes with a pendant thiol moiety.[48] We would like to remind the reader that $\{MNO\}^n$ is the Enemark–Feltham notation, used to avoid assigning oxidation states in transition-metal nitric oxide (NO) complexes. The exponent "*n*" counts the total number of metal (d) and NO (π^*) electrons.[49]

2.3 Gas phase

In a work in progress, we describe a new procedure for HNO generation in the gas phase, which consists of the heterogeneous phase reaction of a base-catalyzed solid HNO donor, (Piloty's acid derivatives and HAPY-1), with a gaseous base, such as ammonia.[50] In this process, which does not need liquid phases or extreme experimental conditions in contrast to previous methods,[51–55] HNO forms after the gaseous base reaches the solid surface and deprotonates the Piloty's acid derivative to give the sulfinite salt, in concordance with the decomposition mechanism in solution. At pressures around 1 bar and room temperature, HNO mainly dimerizes to yield water and N_2O (eqn (1)), whose FT-IR signal can be detected once it has left the solid's surface. HNO generation could also be assessed by two different mass spectrometry methods.

Kinetic measurements suggest that HNO production rate is affected by diffusion processes inside the solid structure, including both the penetration of the gaseous base and the escaping of the formed HNO into the gas phase. Although the overall kinetic process is somewhat complex, a rapid initial growth is observed during the first seconds, followed by a slower, linear growth. The first process is considered to be mainly dependent on gas-phase diffusion and mixing processes as well as the gaseous base's adsorption rate. Once an equilibrium base concentration has been reached over the solid's surface, N_2O concentration begins to grow linearly until the available sites on the surface begin to become scarce. Surprisingly, the kinetic constant associated to the first process, 7×10^{-2} s^{-1}, is similar to that obtained for HNO generation in solution from Piloty's acid derivatives at basic pH (4.4×10^{-2} s^{-1}),[56] and both could be fitted to a first-order regime. The reaction appears to be mostly a superficial process, with little diffusion of the gaseous base into the solid particles, since the N_2O production yield was calculated as approximately 25% *via* FT-IR and NMR spectroscopic measurements, and so most of the solid remains unreactive. The synthesis and use of nanoparticulated Piloty's acid derivatives could therefore cause a dramatic increase in HNO production yield.

This economic and straightforward method for azanone generation in the gas phase may allow deepening the study of HNO gas-phase chemistry, and analyze, for example, its reactivity towards oxygen, which has remained an issue of certain controversy. In solution, while peroxynitrite has been proposed as a product for this reaction by some authors, others claim that NO$^\bullet$ and the hydroperoxide radical are formed instead.[57,58] The high reactivity of either possible species prevents more detailed studies, and so this new clean generation method in the gas phase might be of much use.[59] Apart from probably allowing new reactivity studies, the controlled generation of HNO can give rise to a new drug delivery scheme for novel treatments, in which azanone may be inhaled instead of administered through donors in solution. In order to achieve these promising applications, of course, an appropriate system is to be constructed, in which the degree of dimerization can be controlled, oxidation is avoided, and, most importantly, the excess gaseous base is properly retained by using selective membranes or acid traps.[60–63] Nitric oxide, for example, has already been successfully used as an inhaled therapeutic agent to treat cardiac as well as respiratory conditions, to the point of reducing the need for assisted respiration in some cases.[64–70]

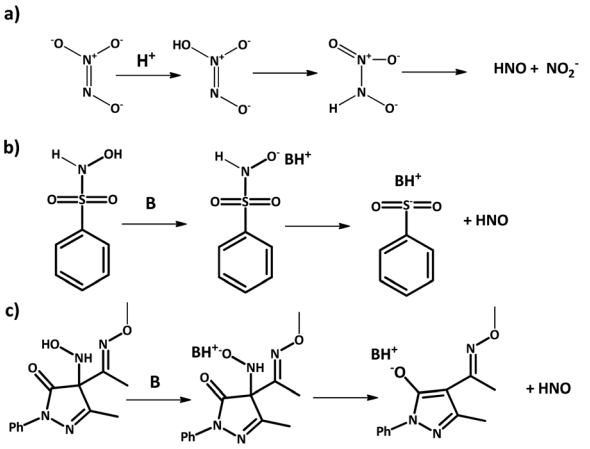

Scheme 3 HNO generation from donors. (a) Angeli's salt; (b) Piloty's acid; (c) HAPY-1.

2.4 Endogenous generation

The endogenous generation of NO$^\bullet$ has been well established, since nitric oxide synthase (NOS), using NADH and dioxygen, generates NO$^\bullet$ and citrulline from the amino acid L-arginine.[71]

Under hypoxic conditions, NO$^{\bullet}$ can also be generated by nitrite reduction mediated by Cu or Fe metalloenzymes.[72] In contrast, the endogenous generation of HNO remains a key question to be answered, in order to understand its possible biological functions. NO$^{\bullet}$ reduction by alcohols, thiols, amines, and H_2S were in fact shown to generate HNO, as discussed in Section 2.1. Other studies suggest that in the absence of the biopterin cofactor, NOS generates HNO from arginine.[73,74]

Additionally, *in vitro* studies demonstrated that the reaction of nitrosothiols (RSNOs) with excess thiols promotes the formation of disulphide and HNO,[75,76] while the reaction between RSNOs and ascorbate produces dehydroascorbate and HNO.[77] The generation of HNO by the action of certain enzymes has also been proposed. For example, Fe or Mn superoxide dismutase (SOD) enzymes produces azanone from NO$^{\bullet}$,[78] while bacterial cytochrome C nitrite reductase catalyses the six-electron reduction of nitrite to ammonium *via* an HNO intermediate, coordinated to an heme centre.[79,80] Moreover, some heme enzymes in the nitrogen cycle, such as Cyt P450nor, are proposed to function *via* HNO intermediates,[81]

In an interdisciplinary approach, taking advantage of selective methods for HNO detection under *in vitro* and intracellular conditions, we suggested that H_2S could transform endogenous NO$^{\bullet}$ into HNO in sensory neurons. These results were surprisingly identical to those observed in stimulation with HNO, observing a clear specific activation of the sensory channel of TRPA1 chemoreceptors through the formation of disulfide bonds in N-terminal cysteines, which activate the HNO-TRPA1-CGRP cascade (TRPA1: transient receptor potential channel A1; CGRP: calcitonin gene-related peptide).[82] The endogenous formation of HNO could be observed using a fluorescent probe, which also showed that HNO production was inhibited by NO$^{\bullet}$ synthase inhibitors and/or cystathionine beta-synthase (CBS) inhibitors.

Another possible source of endogenous HNO is based on the oxidation of different nitrogen containing species mediated by several hemoproteins, which are capable of stabilizing oxo-ferryl species, such as peroxidases.[83–85] For example, we confirmed that myoglobin produces HNO *via* the peroxidation of hydroxylamine with excellent catalytic activity.[86]

Another proposal for the production of HNO *in vivo* results from the enzymatic activity of nitric oxide synthases (NOS) under particular conditions such as the absence of its biopterin cofactor.[74] Other non-enzymatic pathways include reactions between biologically relevant molecules with NO$^{\bullet}$, such as those named above, which lead to the formation of HNO and suggest its possible endogenous formation. However, this has not been definitively confirmed due to difficulties in unequivocal detection of HNO. In a collaborative work currently in progress, we determined the generation of HNO in human platelet-rich plasma using the electrochemical HNO sensor developed by our group. The results show the effective formation of HNO in platelets, after stimulating them with the addition of agonists such as adenosine diphosphate (ADP) and a synthetic peptide agonist of the PAR-1 thrombin receptor called PAR1-AP.[87,88] Currently, HNO detection in this biological system is under study, using a selective phosphine-based fluorescent probe.[89]

3. Stabilization by metalloporphyrins and other ligands

3.1 Metalloporphyrins

Given the high reactivity of free HNO, researchers have tried to stabilize azanone and its conjugate base, NO^-, by coordination to a metal center using a variety of ligands. In particular, heme proteins and synthetic porphyrins have been consistently explored due to the special biological relevance of such biomimetic complexes, which may resemble reactive intermediates in the reaction mechanisms of certain enzymes of the nitrogen cycle. Moreover, the interaction of HNO with heme active sites is closely related to the physiological effects exhorted by this gasotransmitter.

Iron porphyrin derivatives are the clear protagonists, since the electronic properties of this metal center allows the formation of $\{FeNO\}^6$, $\{FeNO\}^7$ and $\{Fe(H)NO\}^8$ complexes which can be interpreted as Fe(II)–NO$^+$, Fe(II)–NO$^{\bullet}$ or Fe(II)–NO$^-$/HNO, and therefore there is a rich redox reactivity to be exploited.[90] In contrast, manganese porphyrins only produce $\{MnNO\}^6$ complexes which are not reduced to the $\{MnNO\}^{7/8}$ forms, whereas cobalt porphyrins form uniquely $\{CoNO\}^8$ species, and oxidation occurs on the porphyrin ring.[91] Attempts to obtain the $\{CoHNO\}^8$ derivatives, however, result in porphyrin ring protonation.[92] Nevertheless, although $\{CoHNO\}^8$ species have not been stabilized, the cationic porphyrin [Co(II)TMPyP]$^{4+}$ has been shown to effectively catalyze the reduction of nitrite to ammonia, and so the formation of a HNO complex could be proposed as an intermediate.[93]

$\{Fe(H)NO\}^8$ complexes might be prepared from their nitrosyl derivatives *via* chemical or electrochemical reduction, or *via* hydride attack on the $\{FeNO\}^6$ species. The pioneering works of Kadish provided the first evidence for $\{FeNO\}^8$ complexes in organic media, *via* spectroelectrochemical studies using TPP (*meso*-tetraphenyl porphyrin) and OEP (β-octaethyl porphyrin);[94,95] they were later obtained by Ryan and coworkers *via* chemical reduction in THF, which enabled their FT-IR characterization.[96,97] More recently, they also succeeded in obtaining the crystal structure of [Fe(II)(OEP)(NO)]$^-$.[98] In the presence of weak acids, evidence for the formation of Fe(II)(OEP)(HNO) (Fig. 1a) was also obtained,[99] and this compound resulted stable for hours with excess phenol acting as the proton source.[100] Abucayon and coworkers could prepare the hexacoordinated Fe(II)(OEP)(HNO)(5-MeIm) by hydride attack on the ferric nitrosyl, and characterize it *via* ^{1}H NMR at low temperature.[101] Interestingly, in fact, this strategy had been previously exploited successfully for the preparation of the first HNO porphyrin complex, which featured Ru as the metal center and could also be characterized by FT-IR and ^{1}H NMR, showing greater stability than its iron analogue.[102]

Using the perhalogenated, electron poor porphyrin $TFPPBr_8$ (2,3,7,8,12,13,17,18-octabromo-5,10,15,20-tetrakis-pentafluorophenyl)porphyrin to prevent oxidation, the first heme-model $\{FeNO\}^8$ complex was isolated in our group *via* chemical reduction of the corresponding $\{FeNO\}^7$ derivative.[103] [Fe(II)$TFPPBr_8$NO]$^-$ (Fig. 1b) resulted indefinitely stable in

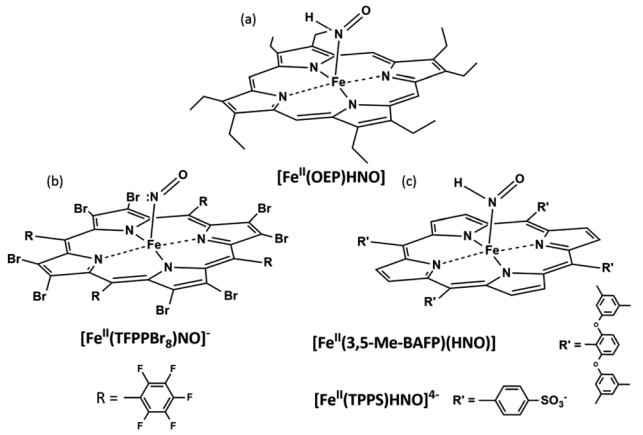

Fig. 1 Fe(II)NO$^-$ and Fe(II)HNO porphyrin complexes.

anoxic solution, and could be characterized *via* UV-Vis, FT-IR and ^{15}N NMR spectroscopies, with this last technique being used for the first time for this kind of compounds. In a more recent work by Hu and Li, even its crystal structure (along with that of the {FeNO}^{7} derivative) could be elucidated.[104] DFT calculations assigned its electronic structure to be intermediate between Fe(II)–NO$^-$ and Fe(I)–NO$^\bullet$, as opposed to non-heme, predominantly Fe(II)–NO$^-$ complexes,[105] as also proposed by Lehnert and coworkers.[106] Despite this complex's remarkable stability, the protonated {Fe**H**NO}^{8} adduct could not be observed, as it immediately yielded the {FeNO}^{7} precursor after acid addition. Reaction (3) with hydrogen production, previously proposed by Choi *et al.*,[96] was therefore considered as a plausible decomposition mechanism in this case.

$$Fe^{II}(P)HNO + H^+ \rightarrow Fe^{II}(P)NO^\bullet + 1/2H_2 \quad (3)$$

This electron-withdrawing platform also allowed for the exploration of a second reduction process, which was found to occur on the porphyrin ring to give a species best described as [{FeNO}^{7}(TFPPBr$_8$)$^{4-}$]$^{2-}$.[107] This electronic configuration would account for the unexpected observed positive shift of ν(NO), that was predicted by DFT calculations, for intermediate- and high-spin states.

Using a sterically hindered bis-picket fence porphyrin, (3,5-Me-BAFP), Lehnert and coworkers could obtain the first HNO ferrous-heme model complex, which, additionally, resulted of great stability with a lifetime of several hours (Fig. 1c).[106] Notably, their results supported the bimolecular decomposition pathway for {Fe**H**NO}^{8} complexes, shown in eqn (4), since it is expected for this reaction to be disfavoured by the presence of the bulky substituents hindering the coordination site.

$$2Fe^{II}(P)HNO \rightarrow 2Fe^{II}(P)NO + H_2 \quad (4)$$

In aqueous media, Lin and Farmer were first successful in stabilizing the HNO adduct of myoglobin, and obtaining its Raman, ^{15}N and ^{1}H NMR, and X-ray absorption spectra.[108,109] This extensive characterization could be accomplished due to the remarkable long lifetime of this complex, which extended over weeks. Other globin-HNO adducts could also be prepared, evidencing the protective nature of the proteic environment.[110]

Almost two decades later, the {FeNO}^{7} derivative of the broadly studied, anionic water-soluble porphyrin TPPS (*meso*-tetraphenylsulphonate porphyrin) could be isolated in our laboratory.[111] More interestingly, the first {FeNO}^{8} and {Fe**H**NO}^{8} derivatives of a water-soluble model could be generated *via* chemical reduction, starting from carefully degassed solutions of the previously isolated Fe(II)–NO$^\bullet$ complex and recrystallized sodium dithionite as the reducing agent.[112] [Fe(II)TPPS(HNO)]$^{4-}$ (Fig. 1c) could be readily obtained at a UV-Vis scale at pH $\leq$ 9, as evidenced by the marked spectral changes, which in turn were consistent with early studies involving flash photolysis reductions of [Fe(II)TPPSNO$^\bullet$]$^{4-}$ generated *in situ*.[113] At more basic pH values, a subtle spectral change was observed after reduction, which suggested the formation of the deprotonated species, [Fe(II)TPPS(NO$^-$)]$^{5-}$; this could be properly confirmed *via* acid-base interconversion experiments. Excitingly, as both species could be identified, the pK_a value for coordinated HNO could be determined as 9.7 *via* electrochemical as well as UV-Vis studies, by monitoring the pH dependence of the reduction potential of [Fe(II)TPPSNO$^\bullet$]$^{4-}$. The reduction potential for {FeNO}^{7}/{FeNO}^{8} was estimated as -0.885 *vs.* Ag/AgCl, while at pH 6, E_{RED} for {FeNO}^{7}, H$^+$/{Fe**H**NO}^{8} was measured as -0.655 V *vs.* Ag/AgCl, in agreement with previous results obtained by Meyer and coworkers using [Fe(II)TPPSNO$^\bullet$]$^{4-}$ prepared *in situ*.[114] Due to the relative stabilization of the NO$^-$ moiety upon coordination, the pK_a value of 9.7 is expectedly lower than the reported value for free HNO.[3] Moreover, the estimated value is in agreement with the one reported for a Ru(II)–HNO complex,[115] and falls in the 8–10 range proposed for Fe(II)OEP(HNO).[100] It is important to note that this is the first pK_a value obtained for a ferrous porphyrin biomimetic complex, suggesting that heme-HNO complexes might exist in the protonated form under physiological conditions.

Although both reduced species eventually reoxidize to the {FeNO}^{7} precursor, the protonated [Fe(II)TPPS(HNO)]$^{4-}$ complex appears to decay faster, as soon as it is formed, following a first order regime. Notably, these results do not agree with the previously proposed bimolecular reaction shown in eqn (4). The observed unimolecular constant, $k = (0.017 \pm 0.003)$ s^{-1}, did not change significantly under a variety of experimental conditions, including pH, although a primary kinetic isotopic effect was observed when the reaction was conducted in D_2O suggesting a rate-limiting step involving H–NO bond breaking. Furthermore, the addition of the H$^\bullet$ abstracting radical TEMPO$^\bullet$ to a cuvette containing freshly formed [Fe(II)TPPS(HNO)]$^{4-}$ resulted in immediate and complete conversion to the {FeNO}^{7} species, further evidencing the relative weakness of the H–NO bond. DFT calculations using the Fe(II)TPP(HNO) model suggested a feasible limiting step involving the migration of the H atom in the HNO moiety to the most proximal *meso* carbon in the porphyrin ligand. As a result, a phlorin radical intermediate is formed, only 2.4 kcal mol^{-1} more energetic than the starting azanone complex (Fig. 2).

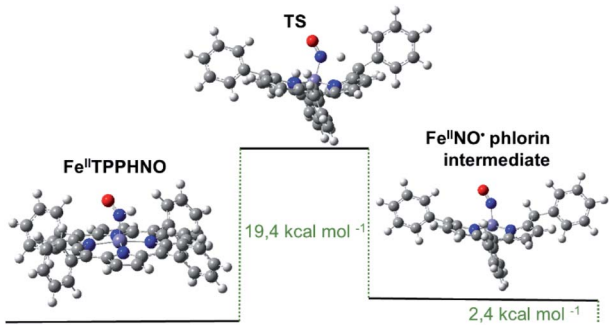

Fig. 2 Optimized structures and calculated energy differences for Fe(II)TPP(HNO), the final phlorin intermediate and transition state.

Additionally, the calculated activation energy for this process fell in the range of the experimentally estimated value. Similar proton-coupled electron transfers for other porphyrins have also been reported in recent works, in which phlorin intermediates were proposed and even detected.[116,117] The obtained results altogether suggest a first-order decomposition mechanism, new for a {Fe**H**NO}^{8} species, involving homolytic H–NO cleavage and phlorin radical formation as the rate-limiting step.

Although new information on {Fe**H**NO}^{8} and {FeNO}^{8} complexes is disclosed every year, these species remain very elusive, and the fundamental reasons for their instability are not yet completely understood. The bimolecular reaction (4) might be a main decomposition pathway in organic media, while its relevance in aqueous media is not apparent from our results. In this case, although steric protection must also be considered, as shown by the fairly inert globin HNO adducts, hydrogen bonding apparently plays a crucial role in stabilizing the HNO moiety, as has been shown in theoretical studies for heme-protein systems.[118,119] This is evidenced by the stability of the water soluble complex $[Fe(II)(CN)_5(HNO)]^{3-}$,[120] and the relatively long lifetime of $[Fe(II)TPPS(HNO)]^{4-}$, a compound based on an unhindered porphyrin in water, as compared to organic-soluble counterparts. The importance of hydrogen bonding has also been recently highlighted by Rahman and Ryan, where they report the existence of an equilibrium between the protonated Fe(II)(OEP)(HNO) complex and the hydrogen bonded Fe(II)(OEP)(NO^-)···H–O–Ph complex in the presence of phenols.[121] The electronic properties and saturation of the porphyrin ring also play determining roles in the reactivity of FeNO porphyrinates, which could even be responsible for the diverse reaction products yielded by different heme-based nitrite reductases, as reported recently by Amanullah and Dey.[122] Evidently, further research should be pursued in all these directions in order to disclose the rich bioinorganic chemistry performed by iron porphyrin nitrosyl and azanone derivatives, which remain a very intriguing field.

3.2 Pincer ligand complexes

There have been no reports thus far of HNO stabilization by complexes with pincer ligands, although some reports of HNO release by these type of nitrosyl species do suggest the existence of intermediate HNO adducts. On the one hand, Caulton and coworkers report of the HNO release from the reaction between an osmium polihydride complex Os(PNP)$(H)_3$ (Fig. 3a) and nitric oxide constitutes of a thorough example.[123] In this reaction, as depicted in eqn (5), the loss of H_2 is a key step which enabled the formation of an intermediate dinitrosyl hydride species (detected by FTIR and XRD) which then undergoes an insertion to form bound HNO. This last species, however, could not be detected, since HNO is reportedly released faster than the adduct is formed.

$$Os(PNP)(H)_3 + 2NO^{\bullet} \rightarrow Os(PNP)(NO) + HNO + H_2 \quad (5)$$

On the other hand, in our laboratory, hydride attack on a {RhNO}^{8} Rh(I)PCPNO$^+$ complex[124] produced the reduced {RhNO}^{9} Rh(I)PCPNO$^{\bullet}$ species,[125] also suggesting the intermediacy of an HNO complex with H_2 production.[126]

NO^- stabilization by complexes with pincer scaffolds is far better known. Several structural analyses of this kind of species exist in bibliography,[124,127–133] along with reports of their catalytic activity.[134–136] Within our group, several rhodium-based pincer ligand systems have been studied (the most relevant are highlighted in Fig. 3b). For such cases the formal assignation of oxidation states is not direct, and, through the use of different techniques, we have concluded that the combined analysis of the ν(NO) FTIR signal along with the XRD-determined value of the Rh–N–O angle is sufficient to identify NO^- configurations.[124] A PCN ligand system proved particularly prone to yield Rh(III)NO^-, even leading to the stabilization of adducts with the weakly-coordinating anions PF_6^- and BF_4^-.[137] Most of our studies on pincer nitrosyls focus on the exploration of their rich redox chemistry.[125,137]

3.3 Other complexes

There have been several studies of HNO/NO^- stabilization for complexes based in multidentate ligands that cannot be formally classified neither as pincers nor porphyrins, albeit similar in structure. Much the same as for iron porphyrins, $FeNO^-$ electronic structures electronic structures are

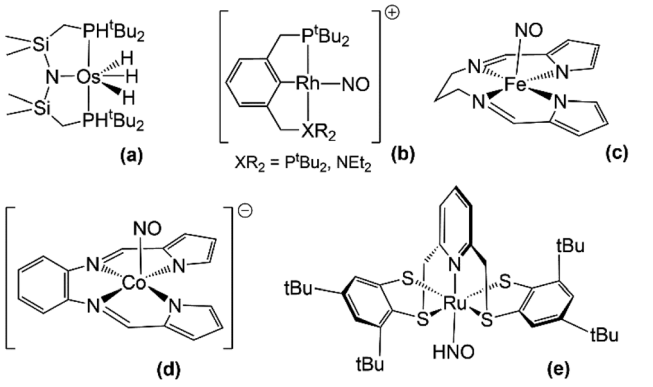

Fig. 3 Some structures of pincer (a and b) and other multidentate–ligand (c–e) complexes relevant to HNO stabilization.

predominant for non-heme iron systems.[138] Worth mentioning are cyclam-based structures[105,139] and some other N-tetracoordinate chelate structures[140–142] which have been found to stabilize NO^- and to release HNO under certain conditions, suggesting the existence of an intermediate M–N(H)O species. Harrop and coworkers have reported a $\{FeNO\}^8$ complex with potential HNO-donor ability (Fig. 3c),[142] which yielded the reductive nitrosylation product of metmyoglobin upon exposure to it and showed inhibition for this same reaction in the presence of glutathione. However, the exact nature of the reactive species could not be verified, and mechanistic details have not yet been reported. In a subsequent work, they also studied the potential of another complex, this time of cobalt with a different type of N-tetracoordinate ligand (Fig. 3d), as an HNO-donor.[141] In this last case, HNO could be trapped both by metmyoglobin and a manganese porphyrin, and could also be indirectly detected by an N_2O FTIR signal (see Section 4.1) when the $\{CoNO\}^9$ species was made to react in water. A Co^{II}–HNO intermediate was putatively proposed to be involved in the release of HNO but could not be isolated. Interestingly, a dinitrosyl species $\{Co(NO)_2\}^{10}$ was also detected in these reactions and was proved to release HNO as well.

On the subject of HNO stabilization, Hess and coworkers' study of a Ru complex with a pentacoordinate ligand is most remarkable, since it is one of the few systems where an HNO adduct could be fully characterized (Fig. 3e).[143] This adduct was obtained by the reaction of $[Ru(py^{bu}S_4)(NO)]^+$ with $NaBH_4$ in methanol at 0 °C, and was characterized by ^1H and ^{13}C NMR, FTIR, mass spectrometry and XRD. Complex $[Ru(py^{bu}S_4)(HNO)]$ was found to be highly reactive. It could not be deprotonated back to its NO^- precursor with Brønsted bases such as triethylamine, butyllithium or lithium methoxide. However, reaction with Brønsted acids ($H_2PO_3^-$, HBr and triflic acid) did yield $[Ru(py^{bu}S_4)(NO)]^+$. This reaction was described as a $2e^-/1H^+$ oxidation and is probably coupled to H_2 formation.

Also of relevance are Slep and coworkers' works based on a family of ruthenium complexes with N-chelating ligands, which notably coordinate HNO.[115,144,145] Moreover, the HNO coordinated species were stable enough for their pK_a for HNO/NO^- conversion to be experimentally obtained, as aforementioned, and clear correlations between HNO acidity and the electronic parameters of the coordination sphere could be established.[144,145]

4. HNO detection methods

4.1 Indirect detection methods

The detection of HNO is a challenging matter due to the molecule's inherent instability towards dimerization (eqn (1)) and its overall short lifetime. Historically, this tendency towards dimerization was exploited as a means to detect HNO through N_2O by CG-MS and FT-IR,[146–148] but later evidence of other azanone-independent mechanisms that could also lead to release of N_2O proved this method to be less reliable.[149,150] Some of the first detection methods that were devised as an alternative were mainly based on HNO trapping with different scavengers and monitoring by either UV-spectrophotometry or EPR. Thus, investigation on HNO trapping became extremely relevant.

One of the most studied HNO traps in bibliography are metalloporphyrins, and our laboratory group has conducted broad research on this subject. Early reports of HNO trapping by these species included both hemoproteins[10,108,151–153] as well as isolated porphyrins.[154] These last type of heme-model systems are a powerful tool, since they essentially retain the reactivity of the hemoprotein active site but allow for a simpler manipulation and reactivity monitoring. In initial works, the trapping kinetics of Fe and Mn porphyrins were reported and it was established that, whereas Fe porphyrins reacted with azanone yielding the same product as for reductive nitrosylation with excess $NO^\bullet$, Mn porphyrins had a much slower reaction -if any- with $NO^\bullet$, therefore being capable of HNO/$NO^\bullet$ discrimination.[155–157] This was further investigated in a separate work where the trapping kinetics of several porphyrins was studied. The work led to the conclusion that manganese-porphyrins with the most negative potentials were the most suitable traps for azanone detection, since they enabled a pathway through free HNO, instead of proceeding *via* a direct donor–porphyrin interaction, together with a large Soret band shift.[158] Other relevant studies were focused on improving the stability of the final trapping product by protecting it from air-induced oxidation, which represented the main limitation of the method. Our group worked on the insertion of the Mn porphyrin in a protein environment,[159] whereas Shoenfisch and co-workers developed a gel-encapsulated Mn porphyrin system, both with great results.[160] However, these colorimetric methods bear the disadvantage of monitoring a wavelength where most biological compounds typically absorb, and so interfere in the detection of azanone for *in vivo* analysis.

Thiols are also optimal for HNO trapping, partly because they have fast kinetics for its reaction with this molecule.[161] It has long been established that the reaction of azanone with thiols leads to the formation of $RS(O)NH_2$, which are very specific products that can be exploited as markers, even enabling HNO/$NO^\bullet$ discrimination.[151,162–166] Although these species have been successfully monitored through NMR,[167] their detection by HPLC-UV is more useful due to its higher inherent sensitivity.[163,166,168] It must be noted, however, that purification is required for UV detection of the marker.

Another successful trapping system, albeit far less frequently reported for its use in colorimetric detection, are phosphines. Most relevant is King and co-workers' study on several phosphine-based traps which includes one of the few reports of an indirect colorimetric method that has enabled quantification of HNO *in vitro*.[169]

As far as EPR-monitoring is concerned, nitronyl nitroxides have been demonstrated to work as efficient paramagnetic probes capable of HNO/$NO^\bullet$ discrimination.[170,171] In particular, their encapsulation in liposomes has been proposed as a means to improve indirect HNO detection.[172] A great advantage of this last method is that it could be suitable for biological systems, since no interference is expected and the reactants are protected from decomposition by the liposome matrix. However, no further experiments have been carried out to date on this

Table 3 Summary of some relevant works on indirect HNO detection

Detection	Trapping system	Advantages	Disadvantages
UV-Vis	Mn-porphyrin in a protein matrix[159]	+ Air stable + Good sensitivity (low nM level) + HNO/NO discrimination	− Limited application in biological samples due to UV Soret band interference
UV-Vis	Mn-porphyrin in a xerogel[160]	+ Air stable + Good sensitivity (low nM level) + HNO/NO discrimination	− Limited application in biological samples due to UV Soret band interference − Cannot be reused due to gel aging
HPLC-UV	Thiol (glutathione)[166]	+ HNO/NO discrimination + Good sensitivity (low μM level) + Can be applied to biological samples	− Requires previous purification − Formation of GSSG may interfere
UV-Vis	Phosphine carbamates[169]	+ Good sensitivity (low μM level) + HNO/NO discrimination	− Limited application in biological samples due to phosphine hydrolysis
EPR	Liposome-encapsulated nitronyl nitroxides[172]	+ Potential compatibility with biological samples (no experiments have been carried out to date) + HNO/NO discrimination	− Requires special and expensive equipment, which is not always readily available

matter. Some other works using iron dithiocarbamates as traps had also been previously reported, but their ability to discriminate between HNO and NO$^{\bullet}$ is limited.[173,174]

Although these indirect methods have allowed a better understanding of the reactivity of the elusive HNO species, they have some significant flaws, mostly concerning their applicability on biological samples (for a summary, see Table 3).

4.2 Direct detection methods: electrochemistry and mass spectrometry

As mentioned before, indirect methods for azanone detection are based on the detection of a certain reaction product formed due to HNO decomposition. However, direct methods for HNO detection have also been developed, which rely on mass spectrometry and electrochemistry.

4.2.1 Mass spectrometry and electrochemical detection. Membrane Inlet Mass Spectrometry (MIMS), is a technique which has been in use since 1963, when Hoch and Kok reported it as a way to detect dissolved gases in liquid phases by using a semipermeable hydrophobic membrane that keeps the liquid phase from entering the mass spectrometer.[175,176]

In 2011 HNO detection by MIMS was achieved by Toscano and coworkers, by adapting a specific sensor for nitric oxide.[177,178] This method allowed the detection of HNO generated from azanone donors by the observation of the fragmented ion (NO^+), whose presence was evidenced by a large peak at *m*/*z* 30. However, it was not always possible to unequivocally observe the signal at *m*/*z* 31. This signal can emerge from HNO generation or from naturally abundant $^{15}NO^{\bullet}$ formed from N_2O fragmentation. N_2O control experiments were performed, and the *m*/*z* 30 to *m*/*z* 31 ratio was found to be 255 : 1. Therefore, if the observed ratio is smaller, it can be considered as evidence for direct HNO production. HNO generation rate produced *via* reaction of solid donors with gaseous ammonia (but not its yield) was found to be dependent on base injection rate. The ion corresponding to the dimerization product, N_2O^+, could also be observed at *m*/*z* 44. Although a detection limit of approximately 50 nM could be reached, additional experiments, such as HNO trapping, are necessary to corroborate the origin of the *m*/*z* 30 signal, since both NO$^{\bullet}$ and fragmentations from N_2O parent ions could also contribute to this signal. Recently, another method was validated for HNO detection which uses a high-pressure (1–1000 mbar) radiofrequency mass spectrometer. Due to a higher temperature of operation and a different setup, HNO dimerization was less favoured in this procedure, giving a very clear signal at *m*/*z* 31 due to HNO generation.[179]

On the other hand, as mentioned earlier, the reactivity of HNO towards synthetic metalloporphyrins containing divalent transition metals has been intensely studied, and so different colorimetric detection techniques mentioned above have been derived. In particular, Co(II) porphyrins, explored as isoelectronic models of protoheme oxygenases,[180] have a high reactivity towards NO$^{\bullet}$(g) to give Co(III)(Por)NO$^-$ in a few minutes.[181] Correspondingly, the same complex is obtained when Co(III) porphyrins react directly with azanone; in contrast, the reaction of Co(III) with NO$^{\bullet}$(g), gives the unstable Co(III)(Por)NO$^{\bullet}$.[182,183] This critical difference in reactivity, added to the ease and efficiency with which thiol derivative porphyrins can be covalently attached to metal electrodes (*e.g.*, gold, silver),[184,185] have allowed the use of cobalt(II) 5,10,15,20-tetrakis[3-(*p*-acetylthiopropoxy)phenyl]porphyrin [Co(P)], as a tool for the electrochemical discrimination between HNO and NO$^{\bullet}$.[186] In this context, our group has developed a specific time-resolved electrochemical sensor for HNO working at the nanomolar level, which is inert towards other biocompatible reactive oxygen and nitrogen oxide species (ROS and RNOS).[187]

This sensor operates at a fixed potential of 0.8 V *vs.* Ag°/AgCl, where [Co(P)] is stable and no current is observed. In the presence of HNO, Co(III)(P)NO$^-$ is produced, which oxidizes to Co(III)(P)NO$^{\bullet}$ under these conditions. The resulting complex is unstable and releases NO$^{\bullet}$, regenerating the original porphyrin

and allowing the cycle to restart (Scheme 4). The current intensity obtained in the experiment is proportional to the amount of HNO present. This method is capable of quantitatively and selectively detecting HNO in real-time, with a linear response in the range 1–1000 nM.[187,188]

The HNO selective time-resolved electrochemical sensor has been used to verify the production of HNO from NO˙ mediated by H_2S,[189] ascorbate, tyrosine, and other alcohols.[31] In addition, it provided clear evidence of the reaction of NO˙ with certain biological aromatic alcohols obtained from food, such as vitamin E, or used as over-the-counter medications, such as aspirin,[32] and allowed to understand the kinetics behind the reactions of NO˙ with thiols to give HNO.[40] A recent study confirmed HNO production by the myoglobin-mediated oxidation of hydroxylamine using this selective sensor.[86]

Compatibility of this sensor with biological media has also been evaluated: for example, HNO detection was achieved after the addition of ascorbate to immunostimulated macrophages.[31]

4.2.2 Comparison with other methods. When *in vivo* measurements for HNO concentrations inside living cells are required, methods based on fluorogenic probes are preferred. Numerous studies on the application of this type of probes in biological environments displaying high selectivity towards HNO and low cytotoxicity have been reported,[161] and their mechanism of action has also been examined in theoretical studies.[190,191]

In 2010, Lippard *et al.* developed the first copper(II)-based fluorescent probe, Cu(II)(BOT1)[11] (BOT1 = BODIPY-triazole 1) for HNO detection (λ_{em} = 526 nm, ϕ = 0.12). One year later, Yao *et al.* reported another probe, coumarin-based Cu(II)(COT1)[190] this time bearing a green-emitting chromophore (λ_{em} = 499 nm, ϕ = 0.63). Although these probes are also sensible to cysteine and ascorbate, the intracellular levels of these reductants in biological media are not enough to generate a fluorescent response comparable to those observed in the presence of HNO. A similar probe, Cu(II)(COET),[191] based on a 7-diethylamine-coumarin fluorophore with a slightly modified chelating site was reported by Yao *et al.* in 2012. In parallel, Lippard and collaborators designed the benzoresorufin based Cu(II)(BRNO1–3) probes for detection of both HNO and NO˙.[192] A few years later, the Cu(II)(HCD) probe based on *N*-(1*H*-1,2,3-triazole-4-yl) methyl-*N*,*N*-di (2-pyridylmethyl)amine was reported by Xing *et al.* to sense HNO and/or H_2S depending on the probe's microenvironment, making it particularly interesting.[193] Finally, a few fluorescent probes for HNO detection emitting in the infrared region were developed, such as dihydroxanthene-based Cu(II)(DHX1) (λ_{em}= 715 nm, ϕ = 0.05) whose emission spectrum does not overlap with other blue or green-emitting probes.[194] This represents a substantial advantage, since they allow the generation of multi-coloured images and the simultaneous monitoring of two or more analytes inside the cell.[195] In the recent years, many other Cu-based fluorescent probes for HNO detection have been developed, which have helped to understand the photophysical properties of these systems.[196,197]

Nitroxide compounds, which are organic compounds bearing an unpaired electron in an NO˙ motif, can also act as fluorogenic species, since they can act as quenchers when bound to a fluorophore. Nitroxides can be oxidized to the oxoammonium cations and are easily reduced by several compounds, including HNO, to yield the corresponding hydroxylamine. For instance, the reaction between TEMPO (2,2,6,6-tetramethyl-1-piperidinyloxyl radical) and HNO gives TEMPOL-H and NO˙ *via* hydrogen abstraction from the HNO moiety.[164] This method was used to design HNO detection probes which are unreactive towards NO˙.[198]

Phosphine-based probes have proven to possess greater selectivity and sensitivity than Cu(II) probes. In this case, the reductive ligation of HNO produces the release of a fluorescent chromophore.[199–201] Recently developed phosphine based probes have also been able to image HNO in tumors,[202] and simultaneously in the Golgi apparatus and mitochondria.[203] Finally, a thiol based probe takes advantage of the special reactivity of HNO towards these groups, allowing its detection with a metal-free structure.[204] For more detail on the structures and mechanism of action of these probes, the reader is referred to a recent review which summarizes the detection of HNO and other gasotransmitters using these fluorescent tools.[205]

In summary, the biological compatibility shown by fluorescent probes and electrochemical sensors give them an advantage for performing *in vivo* measurements, while MIMS requires the use of complementary techniques to ensure the unequivocal detection of HNO. On the other hand, the fact that most of the fluorogenic probes are based on the one-electron reducing nature of HNO can lead to possible interferences from biological reducing agents such as thiols or ascorbate. In contrast, the externally applied potential in the electrochemical sensor avoids this inconvenience, since the metal centre oxidation state is fixed as Co(III). HNO detection methods are summarised in Fig. 4.

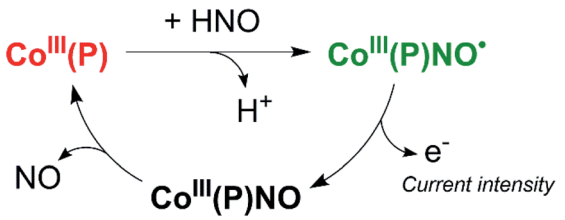

Scheme 4 Reactions Involved in the amperometrical detection of HNO by Co(P).

Perspectives and outlook

Less than ten years ago it was thought that NO˙ was impossible to reduce to HNO by biological agents. This has been assessed not only by state-of-the-art theoretical calculations, but also by showing experimentally that NO˙ can be reduced to HNO by mild reducing agents found in biological media, such as: aromatic and pseudo-aromatic alcohols, including Vitamins C and E, and medicaments such as aspirin, piroxicam and paracetamol.[32] Thiols, H_2S and HS^- also produce HNO, at a faster rate, and aliphatic amines react slow at room temperature and ambient pressure. Therefore, not only HNO can be produced by

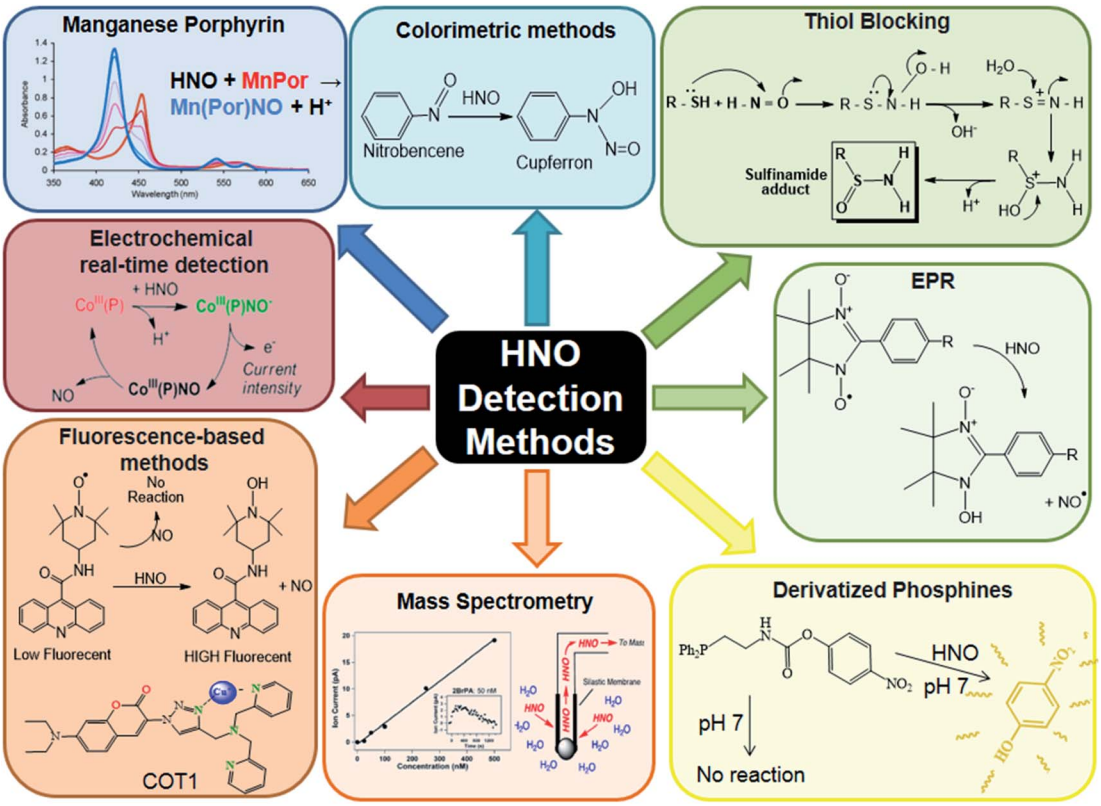

Fig. 4 HNO detection methods. Reproduced from ref. 211.

these agents, but would allow the persistence of HNO in reducing biological environments once produced by nitric oxide reduction or other reactions, and its transportation in free form. Azanone could even be transported, for example, by reduced hemes present in the body.[111] Moreover, HNO endogenous formation is not only a possibility, but a reality: it has been observed to form spontaneously by human platelet aggregation.[87,88,206]

All these findings were made thanks to the use of HNO trapping with metalloporphyrins (an indirect method),[155] and the use of an electrochemical HNO sensor developed in 2013,[187] which allows the direct HNO detection in real time, allowing to obtain kinetic data.

The mechanistic issues related to NO˙ reduction and HNO formation are still open: recent findings suggest the possibility of two successive additions of NO to the RXH substrate, or even the direct reaction with the dimer $(NO)_2$.[207] On one hand, known reactions of NO˙ such as its oxidation with O_2,[208] and its reaction with SO_3^{2-},[209] are thought to proceed through this type of mechanism. On the other hand, it has been found that the formation of $(NO)_2$ is favored in the presence of aromatic rings or negatively charged molecules such as CH_3S^-.[5] Moreover, the reaction of S^{2-} with $(NO)_2$ is exothermic by as much as 84 kcal mol^{-1}, as shown by theoretical calculations.[207] Although S^{2-} is not present at measurable concentration in aqueous solutions, even at high pH values, the reaction could be carried out in organic solvents or by reaction of solid Na_2S with NO. This is not a biologically relevant issue, but a chemical one: the product would be "Thio-Angeli's salt" ON=NSO^{2-}, which can be expected to be a new HNO donor, such as the well-known Angeli's salt (ON=NO$_2^{2-}$).

Regarding medical uses, HNO dimerizes in solution, but in gas phase at low concentrations that reaction is expected to be slow. Therefore, it could be used for respiratory treatments (nowadays NO˙ is used for COVID-19 infections and other pulmonary diseases) or heart treatment: Bristol–Myers–Squibb is developing HNO donors to avoid cardiac arrest.[210] Moreover, the chemistry of HNO(g) is not well known. Since the N–H bond is weak, it could produce NO˙ in the gas phase at low pressures. Therefore, both HNO and NO˙ would be administered with just one solid HNO donor, by reaction with a gas such as NH_3, ethylamine, or HCl, which could be easily removed by a trapping agent.[179]

In summary, azanone arrived to the scene to be the non-radical and reducing offspring of nitric oxide, with properties which are different from his father's, but quite interesting and potentially useful, no doubt at all.

Author contributions

CMG, AM and PV: investigation and writing – original draft; SS, JP and FD: writing-review & editing; FD: conceptualization and supervision.

Conflicts of interest

There are no conflicts to declare.

Acknowledgements

The acknowledgements come at the end of an article after the conclusions and before the notes and references. The research reported in this publication was supported by the Ministerio de Ciencia y Tecnología e Innovación Productiva (PICT-2015-3854 and PICT-2017-1930) and the Universidad de Buenos Aires (UBACYT) project # 20020170100595BA. All authors are CONICET members. C. G., A. M., and P. V. are doctoral students, while S. S., J. P. and F. D. are faculty researchers.

Notes and references

1 L. J. Ignarro, G. M. Buga, K. S. Wood, R. E. Byrns and G. Chaudhuri, *Proc. Natl. Acad. Sci.*, 1987, **84**, 9265–9269.
2 S. Moncada, R. M. Palmer and E. A. Higgs, *Pharmacol. Rev.*, 1991, **43**, 109–142.
3 V. Shafirovich and S. V. Lymar, *Proc. Natl. Acad. Sci. U. S. A.*, 2002, **99**, 7340.
4 D. Srivastava, C. H. Turner, E. E. Santiso and K. E. Gubbins, *J. Phys. Chem. B*, 2018, **122**, 3604–3614.
5 Y.-L. Zhao, M. D. Bartberger, K. Goto, K. Shimada, T. Kawashima and K. N. Houk, *J. Am. Chem. Soc.*, 2005, **127**, 7964–7965.
6 J. Ivanic, M. W. Schmidt and B. Luke, *J. Chem. Phys.*, 2012, **137**, 214316.
7 S. V. Lymar, V. Shafirovich and G. A. Poskrebyshev, *Inorg. Chem.*, 2005, **44**, 5212–5221.
8 J. R. B. Gomes, M. D. M. C. Ribeiro da Silva and M. A. V. Ribeiro da Silva, *J. Phys. Chem. A*, 2004, **108**, 2119–2130.
9 B. Lopez, M. Shinyashiki, T. Han and J. Fukuto, *Free Radicals Biol. Med.*, 2007, **42**, 482–491.
10 D. A. Bazylinski and T. C. Hollocher, *J. Am. Chem. Soc.*, 1985, **107**, 7982–7986.
11 J. Rosenthal and S. J. Lippard, *J. Am. Chem. Soc.*, 2010, **132**, 5536–5537.
12 J. M. Fukuto, A. J. Hobbs and L. J. Ignarro, *Biochem. Biophys. Res. Commun.*, 1993, **196**, 707–713.
13 R. Smulik-Izydorczyk, A. Mesjasz, A. Gerbich, J. Adamus, R. Michalski and A. Sikora, *Nitric Oxide*, 2017, **69**, 61–68.
14 M. I. Jackson, T. H. Han, L. Serbulea, A. Dutton, E. Ford, K. M. Miranda, K. N. Houk, D. A. Wink and J. M. Fukuto, *Free Radicals Biol. Med.*, 2009, **47**, 1130–1139.
15 M. Venâncio, F. Doctorovich and W. Rocha, *J. Phys. Chem. B*, 2017, **121**, 6618–6625.
16 N. Paolocci, M. I. Jackson, B. E. Lopez, K. Miranda, C. G. Tocchetti, D. A. Wink, A. J. Hobbs and J. M. Fukuto, *Pharmacol. Ther.*, 2007, **113**, 442–458.
17 F. L. M. Ricciardolo, P. J. Sterk, B. Gaston and G. Folkerts, *Physiol. Rev.*, 2004, **84**, 731–765.
18 E. G. DeMaster, F. N. Shirota and H. T. Nagasawa, *Alcohol*, 1985, **2**, 117–121.
19 J. Fukuto, P. Gulati and H. T. Nagasawa, *Biochem. Pharmacol.*, 1994, **47**, 922–924.
20 J. C. Irvine, R. H. Ritchie, J. L. Favaloro, K. L. Andrews, R. E. Widdop and B. K. Kemp-Harper, *Trends Pharmacol. Sci.*, 2008, **29**, 601–608.
21 P. Ramakrishnan Geethakumari, M. J. Schiewer, K. E. Knudsen and Wm. K. Kelly, *Curr. Treat. Option On.*, 2017, **18**, 37.
22 J. Galizia, M. P. Acosta, E. Urdániz, M. A. Martí and M. Piuri, *Tuberculosis*, 2018, **109**, 35–40.
23 P. Pagliaro, D. Mancardi, R. Rastaldo, C. Penna, D. Gattullo, K. M. Miranda, M. Feelisch, D. A. Wink, D. A. Kass and N. Paolocci, *Free Radicals Biol. Med.*, 2003, **34**, 33–43.
24 B. K. Kemp-Harper, J. D. Horowitz and R. H. Ritchie, *Drugs*, 2016, **76**, 1337–1348.
25 J. C. Hartman, C. L. del Rio, J. E. Reardon, K. Zhang and H. N. Sabbah, *JACC*, 2018, **3**, 625–638.
26 S. R. Roof, Y. Ueyama, R. Mazhari, R. L. Hamlin, J. C. Hartman, M. T. Ziolo, J. E. Reardon and C. L. del Rio, *Front. Physiol.*, 2017, **8**, 894.
27 C. X. Qin, J. Anthonisz, C. H. Leo, N. Kahlberg, A. Velagic, M. Li, E. Jap, O. L. Woodman, L. J. Parry, J. D. Horowitz, B. K. Kemp-Harper and R. H. Ritchie, *Antioxid. Redox Signaling*, 2020, **32**, 60–77.
28 D. J. Carlsson, R. Brousseau, C. Zhang and D. M. Wiles, *Polyolefin oxidation: Quantification of alcohol and hydroperoxide products by nitric oxide reactions*, 1987, vol. 17.
29 M. Graetzel, S. Taniguchi and A. Henglein, *Ber. Bunsen-Ges.*, 1970, **74**, 1003–1010.
30 W. Pryor, D. Church and C. Govindan, *J. Org.*, 1982, 156–159.
31 S. A. Suarez, N. I. Neuman, M. Muñoz, L. Álvarez, D. E. Bikiel, C. D. Brondino, I. Ivanović-Burmazović, J. Lj. Miljkovic, M. R. Filipovic, M. A. Martí and F. Doctorovich, *J. Am. Chem. Soc.*, 2015, **137**, 4720–4727.
32 M. Hamer, S. A. Suarez, N. I. Neuman, L. Alvarez, M. Muñoz, M. A. Marti and F. Doctorovich, *Inorg. Chem.*, 2015, **54**, 9342–9350.
33 F. Doctorovich, D. Bikiel, J. Pellegrino, S. A. Suárez, A. Larsen and M. A. Martí, *Coord. Chem. Rev.*, 2011, **255**, 2764–2784.
34 Q. C. Yong, S. W. Lee, C. S. Foo, K. L. Neo, X. Chen and J.-S. Bian, *Am. J. Physiol.: Heart Circ. Physiol.*, 2008, **295**, H1330–H1340.
35 J. W. Elrod, J. W. Calvert, J. Morrison, J. E. Doeller, D. W. Kraus, L. Tao, X. Jiao, R. Scalia, L. Kiss, C. Szabo, H. Kimura, C.-W. Chow and D. J. Lefer, *Proc. Natl. Acad. Sci.*, 2007, **104**, 15560–15565.
36 I. Ivanovic-Burmazovic and M. R. Filipovic, *Inorg. Chem.*, 2019, **58**, 4039–4051.
37 M. M. Cortese-Krott, G. G. C. Kuhnle, A. Dyson, B. O. Fernandez, M. Grman, J. F. DuMond, M. P. Barrow, G. McLeod, H. Nakagawa, K. Ondrias, P. Nagy, S. B. King, J. E. Saavedra, L. K. Keefer, M. Singer, M. Kelm, A. R. Butler and M. Feelisch, *Proc. Natl. Acad. Sci.*, 2015, **112**(34), E4651–E4660.
38 J. P. Marcolongo, M. F. Venâncio, W. R. Rocha, F. Doctorovich and J. A. Olabe, *Inorg. Chem.*, 2019, **58**, 14981–14997.

39 S. A. Suarez, P. Vargas and F. A. Doctorovich, *J. Inorg. Biochem.*, 2021, **216**, 111333.
40 S. A. Suarez, M. Muñoz, L. Alvarez, M. F. Venâncio, W. R. Rocha, D. E. Bikiel, M. A. Marti and F. Doctorovich, *J. Am. Chem. Soc.*, 2017, **139**, 14483–14487.
41 M. Hamer, S. Suarez, M. Muñoz, L. Álvarez, M. Marti and F. Doctorovich, *Pure Appl. Chem.*, 2020, **92**(12), 2005–2014.
42 C. T. Aravindakumar, M. De Ley and J. Ceulemans, *J. Chem. Soc., Perkin Trans. 2*, 2002, 663–669.
43 G. Carrone, J. Pellegrino and F. Doctorovich, *Chem. Commun.*, 2017, **53**, 5314–5317.
44 Y. Zhou, R. B. Cink, R. S. Dassanayake, A. J. Seed, N. E. Brasch and P. Sampson, *Angew. Chem.*, 2016, **128**, 13423–13426.
45 Y. Zhou, R. B. Cink, Z. A. Fejedelem, M. Cather Simpson, A. J. Seed, P. Sampson and N. E. Brasch, *Eur. J. Org. Chem.*, 2018, **2018**, 1745–1755.
46 Y. Zhou, R. B. Cink, A. J. Seed, M. C. Simpson, P. Sampson and N. E. Brasch, *Org. Lett.*, 2019, **21**, 1054–1057.
47 M. Kawaguchi, T. Tani, R. Hombu, N. Ieda and H. Nakagawa, *Chem. Commun.*, 2018, **54**, 10371–10374.
48 C.-K. Chiang, K.-T. Chu, C.-C. Lin, S.-R. Xie, Y.-C. Liu, S. Demeshko, G.-H. Lee, F. Meyer, M.-L. Tsai, M.-H. Chiang and C.-M. Lee, *J. Am. Chem. Soc.*, 2020, **142**, 8649–8661.
49 J. H. Enemark and R. D. Feltham, *Coord. Chem. Rev.*, 1974, **13**, 339–406.
50 G. Carrone, A. Mazzeo, E. Marceca, J. Pellegrino, J. Zarenkiewicz, J. P. Toscano and F. Doctorovich, *J. Inorg. Biochem.*, 2021, 111535.
51 M. Bodenstein, *Angew. Chem.*, 1927, **40**, 174–177.
52 P. Harteck, *Ber. Dtsch. Chem. Ges.*, 1933, **66**, 423–426.
53 A. v. Nagel, *Zeitschrift für Elektrochemie und angewandte physikalische Chemie*, 1930, **36**, 754–757.
54 M. a. A. Clyne and B. A. Thrush, *Trans. Faraday Soc.*, 1961, **57**, 69–78.
55 M. a. A. Clyne and B. A. Thrush, *Discuss. Faraday Soc.*, 1962, **33**, 139–148.
56 K. Sirsalmath, S. A. Suárez, D. E. Bikiel and F. Doctorovich, *J. Inorg. Biochem.*, 2013, **118**, 134–139.
57 M. G. Bryukov, A. A. Kachanov, R. Timonnen, J. Seetula, J. Vandoren and O. M. Sarkisov, *Chem. Phys. Lett.*, 1993, **208**, 392–398.
58 R. Smulik, D. Dębski, J. Zielonka, B. Michałowski, J. Adamus, A. Marcinek, B. Kalyanaraman and A. Sikora, *J. Biol. Chem.*, 2014, **289**, 35570–35581.
59 M. Hamer, M. A. Morales Vásquez and F. Doctorovich, in *The Chemistry and Biology of Nitroxyl (HNO)*, ed. F. Doctorovich, P. J. Farmer and M. A. Marti, Elsevier, Boston, 2017, pp. 1–9.
60 P. Wang and T.-S. Chung, *J. Membr. Sci.*, 2015, **474**, 39–56.
61 Z. Ding, L. Liu, Z. Li, R. Ma and Z. Yang, *J. Membr. Sci.*, 2006, **286**, 93–103.
62 Z. Xie, T. Duong, M. Hoang, C. Nguyen and B. Bolto, *Water Res.*, 2009, **43**, 1693–1699.
63 M. S. EL-Bourawi, M. Khayet, R. Ma, Z. Ding, Z. Li and X. Zhang, *J. Membr. Sci.*, 2007, **301**, 200–209.
64 R. A. Krasuski, J. J. Warner, A. Wang, J. K. Harrison, V. F. Tapson and T. M. Bashore, *J. Am. Coll. Cardiol.*, 2000, **36**, 2204–2211.
65 E. Öztürk, S. Haydin, İ. C. Tanıdır, İ. Özyılmaz, Y. Ergül, E. Erek, A. Güzeltaş, E. Ödemiş and İ. Bakır, *Turk Kardiyol Dern Ars*, 2016, **44**, 196–202.
66 United States Patent, *6358536-Nitric oxide donor compositions, methods, apparatus, and kits for preventing or alleviating vasoconstriction or vasospasm in a mammal*, 2002.
67 J. Á. Monsalve-Naharro, E. Domingo-Chiva, S. García Castillo, P. Cuesta-Montero and J. M. Jiménez-Vizuete, *Farm. Hosp.*, 2017, **41**, 292–312.
68 H. Gerlach, D. Pappert, K. Lewandowski, R. Rossaint and K. J. Falke, *Intensive Care Med.*, 1993, **19**, 443–449.
69 L. Chen, P. Liu, H. Gao, B. Sun, D. Chao, F. Wang, Y. Zhu, G. Hedenstierna and C. G. Wang, *Clin. Infect. Dis.*, 2004, **39**, 1531–1535.
70 A. P. Hunt, A. E. Batka, M. Hosseinzadeh, J. D. Gregory, H. K. Haque, H. Ren, M. E. Meyerhoff and N. Lehnert, *ACS Catal.*, 2019, **9**, 7746–7758.
71 D. J. Stuehr, *Annu. Rev. Pharmacol. Toxicol.*, 1997, **37**, 339–359.
72 A. Machha and A. N. Schechter, *Nutr. Rev.*, 2012, **70**, 367–372.
73 Y. Ishimura, Y. T. Gao, S. P. Panda, L. J. Roman, B. S. S. Masters and S. T. Weintraub, *Biochem. Biophys. Res. Commun.*, 2005, **338**, 543–549.
74 H. H. H. W. Schmidt, H. Hofmann, U. Schindler, Z. S. Shutenko, D. D. Cunningham and M. Feelisch, *Proc. Natl. Acad. Sci.*, 1996, **93**, 14492–14497.
75 D. R. Arnelle and J. S. Stamler, *Arch. Biochem. Biophys.*, 1995, **318**, 279–285.
76 L. V. Ivanova, D. Cibich, G. Deye, M. R. Talipov and Q. K. Timerghazin, *ChemBioChem*, 2017, **18**, 726–738.
77 M. Kirsch, A.-M. Büscher, S. Aker, R. Schulz and H. de Groot, *Org. Biomol. Chem.*, 2009, **7**, 1954–1962.
78 D. a. Wink, J. a Cook, S. Y. Kim, Y. Vodovotz, R. Pacelli, M. C. Krishna, a Russo, J. B. Mitchell, D. Jourd'heuil, a M. Miles and M. B. Grisham, *J. Biol. Chem.*, 1997, **272**, 11147–11151.
79 D. Bykov, M. Plog and F. Neese, *JBIC, J. Biol. Inorg. Chem.*, 2014, **19**, 97–112.
80 O. Einsle, A. Messerschmidt, R. Huber, P. M. H. Kroneck and F. Neese, *J. Am. Chem. Soc.*, 2002, **124**, 11737–11745.
81 N. Lehnert, H. T. Dong, J. B. Harland, A. P. Hunt and C. J. White, *Nat. Rev. Chem.*, 2018, **2**, 278–289.
82 M. Eberhardt, M. Dux, B. Namer, J. Miljkovic, N. Cordasic, C. Will, T. I. Kichko, J. de la Roche, M. Fischer, S. A. Suárez, D. Bikiel, K. Dorsch, A. Leffler, A. Babes, A. Lampert, J. K. Lennerz, J. Jacobi, M. A. Martí, F. Doctorovich, E. D. Högestätt, P. M. Zygmunt, I. Ivanovic-Burmazovic, K. Messlinger, P. Reeh and M. R. Filipovic, *Nat. Commun.*, 2014, **5**, 1–17.
83 K. M. Miranda, R. W. Nims, D. D. Thomas, M. G. Espey, D. Citrin, M. D. Bartberger, N. Paolocci, J. M. Fukuto, M. Feelisch and D. A. Wink, *J. Inorg. Biochem.*, 2003, **93**, 52–60.

84 M. G. Espey, K. M. Miranda, D. D. Thomas and D. A. Wink, *Free Radicals Biol. Med.*, 2002, **33**, 827–834.
85 J. A. Reisz, E. Bechtold and S. B. King, *Dalton Trans.*, 2010, **39**, 5203–5212.
86 L. Álvarez, S. A. Suárez, P. J. González, C. D. Brondino, F. Doctorovich and M. A. Martí, *Inorg. Chem.*, 2020, DOI: 10.1021/acs.inorgchem.9b02750.
87 M. C. Maccaferro, S. B. Suárez Freire, S. Suárez, M. A. Martí, P. C. Ivani, M. A. Schattner and R. G. Pozner, presented in part at the *XIII Congreso Argentino de Hemostasia y Trombosis y IV Curso Educacional de la ISTH*, Buenos Aires, September, 2018.
88 Y. Doctorovich, S. Suárez, F. Doctorovich, M. Schattner and R. Pozner, *XIV Congreso*, Argentino de Hemostasia y Trombosis, Buenos Aires, 2021.
89 Z. Miao, J. A. Reisz, S. M. Mitroka, J. Pan, M. Xian and S. B. King, *Bioorg. Med. Chem. Lett.*, 2015, **25**, 16–19.
90 A. L. Speelman and N. Lehnert, *Acc. Chem. Res.*, 2014, **47**, 1106–1116.
91 E. Fujita, C. K. Chang and J. Fajer, *J. Am. Chem. Soc.*, 1985, **107**, 7665–7669.
92 M. A. Rhine, A. V. Rodrigues, R. J. B. Urbauer, J. L. Urbauer, T. L. Stemmler and T. C. Harrop, *J. Am. Chem. Soc.*, 2014, **136**, 12560–12563.
93 S.-H. Cheng and Y. Su, *Inorg. Chem.*, 1994, **33**, 5847–5854.
94 D. Lancon and K. M. Kadish, *J. Am. Chem. Soc.*, 1983, **105**, 5610–5617.
95 L. W. Olson, D. Schaeper, D. Lancon and K. M. Kadish, *J. Am. Chem. Soc.*, 1982, **104**, 2042–2044.
96 I. K. Choi, Y. Liu, D. W. Feng, K. J. Paeng and M. D. Ryan, *Inorg. Chem.*, 1991, **30**, 1832–1839.
97 Z. Wei and M. D. Ryan, *Inorg. Chem.*, 2010, **49**, 6948–6954.
98 N. Kundakarla, S. Lindeman, Md. H. Rahman and M. D. Ryan, *Inorg. Chem.*, 2016, **55**, 2070–2075.
99 Y. Liu and M. D. Ryan, *J. Electroanal. Chem.*, 1994, **368**, 209–219.
100 Md. H. Rahman and M. D. Ryan, *Inorg. Chem.*, 2017, **56**, 3302–3309.
101 E. G. Abucayon, R. L. Khade, D. R. Powell, Y. Zhang and G. B. Richter-Addo, *J. Am. Chem. Soc.*, 2016, **138**, 104–107.
102 J. Lee and G. B. Richter-Addo, *J. Inorg. Biochem.*, 2004, **98**, 1247–1250.
103 J. Pellegrino, S. E. Bari, D. E. Bikiel and F. Doctorovich, *J. Am. Chem. Soc.*, 2010, **132**, 989–995.
104 B. Hu and J. Li, *Angew. Chem., Int. Ed.*, 2015, **54**, 10579–10582.
105 R. G. Serres, C. A. Grapperhaus, E. Bothe, E. Bill, T. Weyhermüller, F. Neese and K. Wieghardt, *J. Am. Chem. Soc.*, 2004, **126**, 5138–5153.
106 L. E. Goodrich, S. Roy, E. E. Alp, J. Zhao, M. Y. Hu and N. Lehnert, *Inorg. Chem.*, 2013, **52**, 7766–7780.
107 J. Pellegrino, R. Hübner, F. Doctorovich and W. Kaim, *Chem.–Eur. J.*, 2011, **17**, 7868–7874.
108 R. Lin and P. J. Farmer, *J. Am. Chem. Soc.*, 2000, **122**, 2393–2394.
109 C. E. Immoos, F. Sulc, P. J. Farmer, K. Czarnecki, D. F. Bocian, A. Levina, J. B. Aitken, R. S. Armstrong and P. A. Lay, *J. Am. Chem. Soc.*, 2005, **127**, 814–815.
110 M. R. Kumar, D. Pervitsky, L. Chen, T. Poulos, S. Kundu, M. S. Hargrove, E. J. Rivera, A. Diaz, J. L. Colón and P. J. Farmer, *Biochemistry*, 2009, **48**, 5018–5025.
111 A. Mazzeo, J. Pellegrino and F. Doctorovich, *J. Am. Chem. Soc.*, 2019, **141**, 18521–18530.
112 C. E. McKenna, W. G. Gutheil and W. Song, *Biochim. Biophys. Acta*, 1991, **1075**, 109–117.
113 H. Seki, M. Hoshino and S. Kounose, *J. Chem. Soc., Faraday Trans.*, 1996, **92**, 2579–2583.
114 M. H. Barley and T. J. Meyer, *J. Am. Chem. Soc.*, 1986, **108**, 5876–5885.
115 N. O. Codesido, T. Weyhermüller, J. A. Olabe and L. D. Slep, *Inorg. Chem.*, 2014, **53**, 981–997.
116 Y. Fang, Y. G. Gorbunova, P. Chen, X. Jiang, M. Manowong, A. A. Sinelshchikova, Y. Yu. Enakieva, A. G. Martynov, A. Yu. Tsivadze, A. Bessmertnykh-Lemeune, C. Stern, R. Guilard and K. M. Kadish, *Inorg. Chem.*, 2015, **54**, 3501–3512.
117 B. H. Solis, A. G. Maher, D. K. Dogutan, D. G. Nocera and S. Hammes-Schiffer, *Proc. Natl. Acad. Sci. U. S. A.*, 2016, **113**, 485–492.
118 L. Yang, Y. Ling and Y. Zhang, *J. Am. Chem. Soc.*, 2011, **133**, 13814–13817.
119 R. L. Khade, Y. Yang, Y. Shi and Y. Zhang, *Angew. Chem., Int. Ed.*, 2016, **55**, 15058–15061.
120 A. C. Montenegro, V. T. Amorebieta, L. D. Slep, D. F. Martín, F. Roncaroli, D. H. Murgida, S. E. Bari and J. A. Olabe, *Angew. Chem., Int. Ed.*, 2009, **48**, 4213–4216.
121 M. H. Rahman, Y. Liu and M. D. Ryan, *Inorg. Chem.*, 2019, **58**, 13788–13795.
122 S. Amanullah and A. Dey, *Chem. Sci.*, 2020, **11**, 5909–5921.
123 J.-H. Lee, H. Fan, M. Pink and K. G. Caulton, *New J. Chem.*, 2007, **31**, 838–840.
124 C. Gaviglio, Y. Ben-David, L. J. Shimon, F. Doctorovich and D. Milstein, *Organometallics*, 2009, **28**, 1917–1926.
125 J. Pellegrino, C. Gaviglio, D. Milstein and F. Doctorovich, *Organometallics*, 2013, **32**, 6555–6564.
126 Unpublished results.
127 A. Y. Verat, M. Pink, H. Fan, B. C. Fullmer, J. Telser and K. G. Caulton, *Eur. J. Inorg. Chem.*, 2008, **2008**, 4704–4709.
128 B. C. Fullmer, M. Pink, H. Fan, X. Yang, M.-H. Baik and K. G. Caulton, *Inorg. Chem.*, 2008, **47**, 3888–3892.
129 E. Fogler, I. Efremenko, M. Gargir, G. Leitus, Y. Diskin-Posner, Y. Ben-David, J. M. L. Martin and D. Milstein, *Inorg. Chem.*, 2015, **54**, 2253–2263.
130 A. M. Tondreau and J. M. Boncella, *Polyhedron*, 2016, **116**, 96–104.
131 D. Himmelbauer, M. Mastalir, B. Stöger, L. F. Veiros, M. Pignitter, V. Somoza and K. Kirchner, *Inorg. Chem.*, 2018, **57**, 7925–7931.
132 D. Himmelbauer, B. Stöger, L. F. Veiros, M. Pignitter and K. Kirchner, *Organometallics*, 2019, **38**, 4669–4678.

133 J. Pecak, W. Eder, B. Stöger, S. Realista, P. N. Martinho, M. J. Calhorda, W. Linert and K. Kirchner, *Organometallics*, 2020, **39**, 2594–2601.
134 A. Choualeb, A. J. Lough and D. G. Gusev, *Organometallics*, 2007, **26**, 3509–3515.
135 E. Fogler, M. A. Iron, J. Zhang, Y. Ben-David, Y. Diskin−Posner, G. Leitus, L. J. W. Shimon and D. Milstein, *Inorg. Chem.*, 2013, **52**, 11469–11479.
136 J. Pecak, B. Stöger, M. Mastalir, L. F. Veiros, L. P. Ferreira, M. Pignitter, W. Linert and K. Kirchner, *Inorg. Chem.*, 2019, **58**, 4641–4646.
137 C. M. Gallego, C. Gaviglio, Y. Ben-David, D. Milstein, F. Doctorovich and J. Pellegrino, *Dalton Trans.*, 2020, **49**, 7093–7108.
138 A. L. Speelman, B. Zhang, C. Krebs and N. Lehnert, *Angew. Chem., Int. Ed.*, 2016, **55**, 6685–6688.
139 D. R. Lang, J. A. Davis, L. G. F. Lopes, A. A. Ferro, L. C. G. Vasconcellos, D. W. Franco, E. Tfouni, A. Wieraszko and M. J. Clarke, *Inorg. Chem.*, 2000, **39**, 2294–2300.
140 L. M. Baltusis, K. D. Karlin, H. N. Rabinowitz, J. C. Dewan and S. J. Lippard, *Inorg. Chem.*, 1980, **19**, 2627–2632.
141 M. R. Walter, S. P. Dzul, A. V. Rodrigues, T. L. Stemmler, J. Telser, J. Conradie, A. Ghosh and T. C. Harrop, *J. Am. Chem. Soc.*, 2016, **138**, 12459–12471.
142 A. K. Patra, K. S. Dube, B. C. Sanders, G. C. Papaefthymiou, J. Conradie, A. Ghosh and T. C. Harrop, *Chem. Sci.*, 2012, **3**, 364–369.
143 D. Sellmann, T. Gottschalk-Gaudig, D. Häußinger, F. W. Heinemann and B. A. Hess, *Chem.–Eur. J.*, 2001, **7**, 2099–2103.
144 N. Levin, N. O. Codesido, J. P. Marcolongo, P. Alborés, T. Weyhermüller, J. A. Olabe and L. D. Slep, *Inorg. Chem.*, 2018, **57**, 12270–12281.
145 J. Perdoménico, M. M. Ruiz, N. O. Codesido, A. G. D. Candia, J. P. Marcolongo and L. D. Slep, *Dalton Trans.*, 2021, **50**, 1641–1650.
146 K. M. Miranda, *Coord. Chem. Rev.*, 2005, **249**, 433–455.
147 H. T. Nagasawa, E. G. DeMaster, B. Redfern, F. N. Shirota and D. J. W. Goon, *J. Med. Chem.*, 1990, **33**, 3120–3122.
148 J. M. Fukuto, M. D. Bartberger, A. S. Dutton, N. Paolocci, D. A. Wink and K. N. Houk, *Chem. Res. Toxicol.*, 2005, **18**, 790–801.
149 J. Y. Cho, A. Dutton, T. Miller, K. N. Houk and J. M. Fukuto, *Arch. Biochem. Biophys.*, 2003, **417**, 65–76.
150 J. Yoo and J. M. Fukuto, *Biochem. Pharmacol.*, 1995, **50**, 1995–2000.
151 M. P. Doyle, S. N. Mahapatro, R. D. Broene and J. K. Guy, Oxidation and reduction of hemoproteins by trioxodinitrate(II), *The role of nitrosyl hydride and nitrite*, accessed 21 July 2020, DOI: 10.1021/ja00210a047.
152 E. H. Lan, B. C. Dave, J. M. Fukuto, B. Dunn, J. I. Zink and J. S. Valentine, *J. Mater. Chem.*, 1999, **9**, 45–53.
153 F. Sulc, C. E. Immoos, D. Pervitsky and P. J. Farmer, *J. Am. Chem. Soc.*, 2004, **126**, 1096–1101.
154 I. Spasojević, I. Batinić-Haberle and I. Fridovich, *Nitric Oxide*, 2000, **4**, 526–533.
155 S. E. Bari, M. A. Martí, V. T. Amorebieta, D. A. Estrin and F. Doctorovich, *J. Am. Chem. Soc.*, 2003, **125**, 15272–15273.
156 M. A. Martí, S. E. Bari, D. A. Estrin and F. Doctorovich, *J. Am. Chem. Soc.*, 2005, **127**, 4680–4684.
157 S. A. Suárez, M. A. Martí, P. M. De Biase, D. A. Estrin, S. E. Bari and F. Doctorovich, *Polyhedron*, 2007, **26**, 4673–4679.
158 L. Álvarez, S. A. Suarez, D. E. Bikiel, J. S. Reboucas, I. Batinić-Haberle, M. A. Martí and F. Doctorovich, *Inorg. Chem.*, 2014, **53**, 7351–7360.
159 I. Boron, S. A. Suárez, F. Doctorovich, M. A. Martí and S. E. Bari, *J. Inorg. Biochem.*, 2011, **105**, 1044–1049.
160 K. P. Dobmeier, D. A. Riccio and M. H. Schoenfisch, *Anal. Chem.*, 2008, **80**, 1247–1254.
161 R. Smulik-Izydorczyk, K. Dębowska, J. Pięta, R. Michalski, A. Marcinek and A. Sikora, *Free Radicals Biol. Med.*, 2018, **128**, 69–83.
162 P. S.-Y. Wong, J. Hyun, J. M. Fukuto, F. N. Shirota, E. G. DeMaster, D. W. Shoeman and H. T. Nagasawa, *Biochemistry*, 1998, **37**, 5362–5371.
163 D. W. Shoeman, F. N. Shirota, E. G. DeMaster and H. T. Nagasawa, *Alcohol*, 2000, **20**, 55–59.
164 K. M. Miranda, N. Paolocci, T. Katori, D. D. Thomas, E. Ford, M. D. Bartberger, M. G. Espey, D. A. Kass, M. Feelisch, J. M. Fukuto and D. A. Wink, *Proc. Natl. Acad. Sci. U. S. A.*, 2003, **100**, 9196.
165 B. Shen and A. M. English, *Biochemistry*, 2005, **44**, 14030–14044.
166 S. Donzelli, M. G. Espey, D. D. Thomas, D. Mancardi, C. G. Tocchetti, L. A. Ridnour, N. Paolocci, S. B. King, K. M. Miranda, G. Lazzarino, J. M. Fukuto and D. A. Wink, *Free Radicals Biol. Med.*, 2006, **40**, 1056–1066.
167 G. Keceli, C. D. Moore, J. W. Labonte and J. P. Toscano, *Biochemistry*, 2013, **52**, 7387–7396.
168 S. Donzelli, M. G. Espey, W. Flores-Santana, C. H. Switzer, G. C. Yeh, J. Huang, D. J. Stuehr, S. B. King, K. M. Miranda and D. A. Wink, *Free Radicals Biol. Med.*, 2008, **45**, 578–584.
169 J. A. Reisz, C. N. Zink and S. B. King, *J. Am. Chem. Soc.*, 2011, **133**, 11675–11685.
170 U. Samuni, Y. Samuni and S. Goldstein, *J. Am. Chem. Soc.*, 2010, **132**, 8428–8432.
171 Y. Samuni, U. Samuni and S. Goldstein, *J. Inorg. Biochem.*, 2013, **118**, 155–161.
172 A. A. Bobko, A. Ivanov and V. V. Khramtsov, *Free Radical Res.*, 2013, **47**, 74–81.
173 Y. Xia, A. J. Cardounel, A. F. Vanin and J. L. Zweier, *Free Radicals Biol. Med.*, 2000, **29**, 793–797.
174 A. M. Komarov, D. A. Wink, M. Feelisch and H. H. H. W. Schmidt, *Free Radicals Biol. Med.*, 2000, **28**, 739–742.
175 G. Hoch and B. Kok, *Arch. Biochem. Biophys.*, 1963, **101**, 160–170.
176 C. Tu, E. R. Swenson and D. N. Silverman, *Free Radicals Biol. Med.*, 2007, **43**, 1453–1457.
177 M. R. Cline, C. Tu, D. N. Silverman and J. P. Toscano, *Free Radicals Biol. Med.*, 2011, **50**, 1274–1279.

178 T. A. Chavez and J. P. Toscano, in *The Chemistry and Biology of Nitroxyl (HNO)*, ed. F. Doctorovich, P. J. Farmer and M. A. Martí, Elsevier, 2017, pp. 255–267.
179 G. Carrone, A. Mazzeo, J. Pellegrino, S. Suárez, E. Marceca, J. Zarenkiewicz, and J. P. Toscano, submitted.
180 W. R. Scheidt and J. L. Hoard, *J. Am. Chem. Soc.*, 1973, **95**, 8281–8288.
181 S. Kelly, D. Lancon and K. M. Kadish, *Inorg. Chem.*, 1984, **23**, 1451–1458.
182 P. J. Farmer and F. Sulc, *J. Inorg. Biochem.*, 2005, **99**, 166–184.
183 F. Roncaroli and R. van Eldik, *J. Am. Chem. Soc.*, 2006, **128**, 8042–8053.
184 K. Shimazu, M. Takechi, H. Fujii, M. Suzuki, H. Saiki, T. Yoshimura and K. Uosaki, *Thin Solid Films*, 1996, **273**, 250–253.
185 T. Akiyama, H. Imahori and Y. Sakata, *Chem. Lett.*, 1994, **23**, 1447–1450.
186 S. A. Suárez, M. H. Fonticelli, A. A. Rubert, E. de la Llave, D. Scherlis, R. C. Salvarezza, M. A. Martí and F. Doctorovich, *Inorg. Chem.*, 2010, **49**, 6955–6966.
187 S. A. Suárez, D. E. Bikiel, D. E. Wetzler, M. A. Martí and F. Doctorovich, *Anal. Chem.*, 2013, **85**, 10262–10269.
188 B. F. Doctorovich, S. A. Suárez and M. F. Martí, *HNO Biosensor*, 2018.
189 M. Eberhardt, M. Dux, B. Namer, J. Miljkovic, N. Cordasic, C. Will, T. I. Kichko, J. de la Roche, M. Fischer, S. A. Suárez, D. Bikiel, K. Dorsch, A. Leffler, A. Babes, A. Lampert, J. K. Lennerz, J. Jacobi, M. A. Martí, F. Doctorovich, E. D. Högestätt, P. M. Zygmunt, I. Ivanovic-Burmazovic, K. Messlinger, P. Reeh and M. R. Filipovic, *Nat. Commun.*, 2014, **5**, 4381.
190 Y. Zhou, K. Liu, J.-Y. Li, Y. Fang, T.-C. Zhao and C. Yao, *Org. Lett.*, 2011, **13**, 1290–1293.
191 Y. Zhou, Y.-W. Yao, J.-Y. Li, C. Yao and B.-P. Lin, *Sens. Actuators, B*, 2012, **174**, 414–420.
192 U.-P. Apfel, D. Buccella, J. J. Wilson and S. J. Lippard, *Inorg. Chem.*, 2013, **52**, 3285–3294.
193 H. Lv, R. Ma, X. Zhang, M. Li, Y. Wang, S. Wang and G. Xing, *Tetrahedron*, 2016, **72**, 5495–5501.
194 A. T. Wrobel, T. C. Johnstone, A. Deliz Liang, S. J. Lippard and P. Rivera-Fuentes, *J. Am. Chem. Soc.*, 2014, **136**, 4697–4705.
195 P. Rivera-Fuentes and S. J. Lippard, *Acc. Chem. Res.*, 2015, **48**, 2927–2934.
196 D. Maiti, A. S. M. Islam, A. Dutta, M. Sasmal, C. Prodhan and M. Ali, *Dalton Trans.*, 2019, **48**, 2760–2771.
197 A. S. M. Islam, M. Sasmal, D. Maiti, A. Dutta, S. Ganguly, A. Katarkar, S. Gangopadhyay and M. Ali, *ACS Appl. Bio Mater.*, 2019, **2**, 1944–1955.
198 M. R. Cline and J. P. Toscano, *J. Phys. Org. Chem.*, 2011, **24**, 993–998.
199 J. A. Reisz, C. N. Zink and S. B. King, *J. Am. Chem. Soc.*, 2011, **133**, 11675–11685.
200 Z. Miao and S. B. King, in *The Chemistry and Biology of Nitroxyl (HNO)*, ed. F. Doctorovich, P. J. Farmer and M. A. Martí, Elsevier, 2017, pp. 225–238.
201 K. Kawai, N. Ieda, K. Aizawa, T. Suzuki, N. Miyata and H. Nakagawa, *J. Am. Chem. Soc.*, 2013, **135**, 12690–12696.
202 Z. Chai, D. Liu, X. Li, Y. Zhao, W. Shi, X. Li and H. Ma, *Chem. Commun.*, 2021, **57**, 5063–5066.
203 H. Wang, C. Liu, Z. He, P. Li, W. Zhang, W. Zhang and B. Tang, *Anal. Chem.*, 2021, **93**, 6551–6558.
204 N. W. Pino, J. Davis, Z. Yu and J. Chan, *J. Am. Chem. Soc.*, 2017, **139**, 18476–18479.
205 J. Alday, A. Mazzeo and S. Suarez, *Inorg. Chim. Acta*, 2020, **510**, 119696.
206 P. C. Ivani, *Tesis de Grado*, Universidad de Buenos Aires. Facultad de Ciencias Exactas y Naturales, 2017.
207 N. I. Neuman, M. F. Venâncio, W. R. Rocha, D. E. Bikiel, S. A. Suárez and F. A. Doctorovich, submitted.
208 D. S. Bohle, *Curr. Opin. Chem. Biol.*, 1998, **2**, 194–200.
209 D. Littlejohn, K. Y. Hu and S. G. Chang, *Inorg. Chem.*, 1986, **25**, 3131–3135.
210 United States Patent, *10517847-Nitroxyl donors with improved therapeutic index*, 2019.
211 F. Doctorovich, D. E. Bikiel, J. Pellegrino, S. A. Suárez and M. A. Martí, *Acc. Chem. Res.*, 2014, **47**(10), 2907–2919.